JACS
JOURNAL OF THE AMERICAN CHEMICAL SOCIETY

Communication

pubs.acs.org/JACS

Preparation of Nanofibrous Metal–Organic Framework Filters for Efficient Air Pollution Control

Yuanyuan Zhang, Shuai Yuan, Xiao Feng, Haiwei Li, Junwen Zhou, and Bo Wang*

Key Laboratory of Cluster Science, Ministry of Education of China, Beijing Key Laboratory of Photoelectronic/Electrophotonic Conversion Materials, School of Chemistry, Beijing Institute of Technology, 5 South Zhongguancun Street, Beijing 100081, P. R. China

Supporting Information

ABSTRACT: Environmental challenges especially air pollution (particulate matter (PM) and toxic gases) pose serious threats to public health globally. Metal–organic frameworks (MOFs) are crystalline materials with high porosity, tunable pore size, and rich functionalities, holding the promise for poisonous pollutants capture. Here, nanocrystals of four unique MOF structures are processed into nanofibrous filters (noted as MOFilter) with high MOF loadings (up to 60 wt %). The MOFilters show high PM removal efficiencies up to 88.33 ± 1.52% and 89.67 ± 1.33% for $PM_{2.5}$ and PM_{10}, respectively, in the hazy environment, and the performance remains largely unchanged over 48 h of continuous filtration. For the first time, the interactions between such porous crystalline material and particulate pollutants were explored. These thin MOFilters can further selectively capture and retain SO_2 when exposed to a stream of SO_2/N_2 mixture, and their hierarchical nanostructures can easily permeate fresh air at high gas flow rate with the pressure drop <20 Pa.

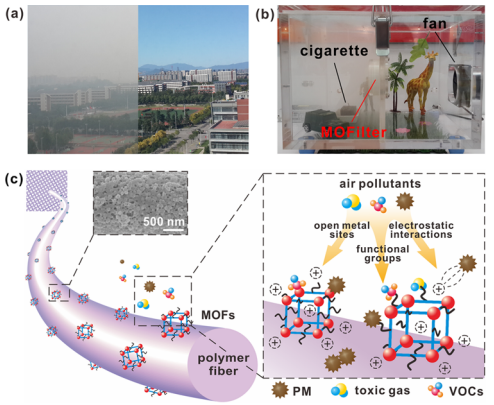

Figure 1. (a) Photos of the campus of the Beijing Institute of Technology during a polluted and a clear day. (b) Demonstration of the particle filtration capability of the MOFilter in the simulated polluted environment. (c) Proposed capture mechanism of the MOFilter for air pollutants. Inset is the SEM image of the surface of the MOF/polymer composite fiber.

With the rapid growth of economy and global industrialization, pollutions especially airborne ones have become one of the most severe threats facing humanity.[1−3] In the practical scenario, air pollutants are highly complicated and can be generally described as particulates, liquid droplets, gases, or mixtures of the above.[4] Among the solid pollutants (i.e., particulate matter, dust, pollen, etc.), fine particulate matter (PM) is the most hazardous one that can have severe influence on public health, air quality, and climate.[5−7] Particulates with aerodynamic diameter below 2.5 μm ($PM_{2.5}$) and 10 μm (PM_{10}) can penetrate into the respiratory system; therefore, long-term exposure to fine particulate matter will lead to many health problems.[5,6] Major gaseous pollutants include sulfur oxides (SO_x), nitrogen oxides (NO_x), carbon monoxide (CO), and chlorofluorocarbons (CFCs). Among them, SO_x (i.e., SO_2) has major negative effects on human health and can cause acid rain and lead to the growth of the PM.[8,9] Figure 1a shows the photos of the campus of the Beijing Institute of Technology during a polluted and clear day, respectively. In such a highly complicated system, air purification becomes even more challenging, and fresh air can be only obtained with high-energy consumption and/or expensive treatment procedures at present.

Air filter is an effective way to purify air at low costs, and various types of filters are in use for the above-mentioned situations. For example, high-efficiency particulate arrestance filters are specially designed for smaller pollutants and particle removal; however, they cannot filter chemical vapors and toxic gases. In another case, large quantities of activated carbon granules are, via a separate adsorption frame, embedded together with the filter system and can be used for volatile organic compounds and toxic gas adsorption. Such arrangement inevitably increases the complexity and cost and may also cause further pressure drop. Therefore, it is a long-sought-after goal to fabricate versatile filters to remove most of the common toxic pollutants, both particles and gaseous species, at the same time.

As one of the emerging porous crystalline materials, metal–organic frameworks (MOFs) are composed of metal ions (or clusters) and organic linkers combining the merits of both organic and inorganic materials.[10−12] Due to the large surface areas, rich functionalities, and high thermal stability, MOFs hold great promise for applications such as gas storage and separation,[13−15] harmful gas capture,[16−26] and adsorption and degradation of chemical warfare agents.[27−29] Moreover, many methods have been proposed to further improve their chemical stability making them more durable in extreme conditions. In practical applications, the powder crystalline materials will cause many

Received: March 9, 2016
Published: April 19, 2016

ACS Publications © 2016 American Chemical Society

DOI: 10.1021/jacs.6b02553
J. Am. Chem. Soc. 2016, 138, 5785−5788

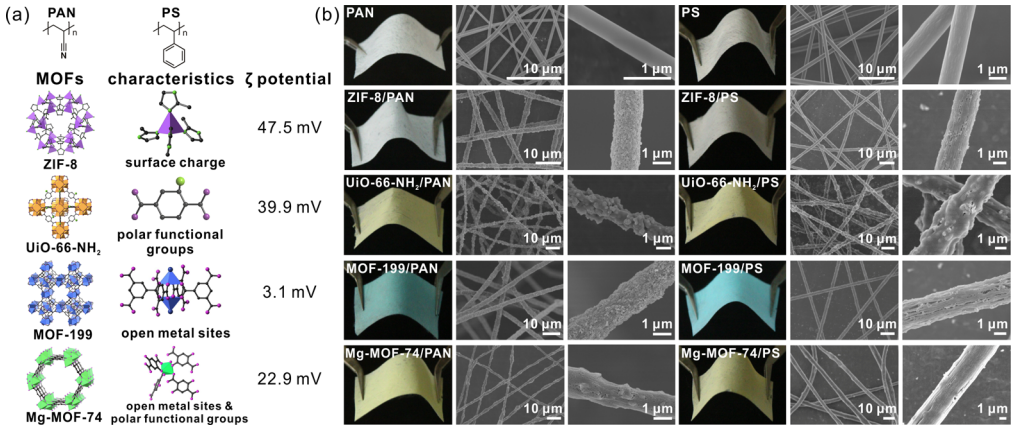

Figure 2. (a) Chemical structures of the polymers, and crystal structures, and ζ potential of the MOFs employed. (b) Photographs and SEM images of the MOFilters (60 wt % MOF loading) supported on nonwoven fabrics.

problems such as clogging of the pipes and/or recycling issues; therefore, it is beneficial to process the powders into films, filters, or shape-bodies. Generally, MOF layers/coatings can be prepared by growing/depositing MOF crystals on porous substrates forming MOF thin films[17,27,30−33] or incorporating MOF particles into polymers (mixed matrix membranes).[33−37]

Electrospinning is a common and facile method to fabricate fibers,[38−41] and some literatures have reported the preparation of electrospun fibers with MOFs as the fillers.[42−46] However, there is no systematic study on processing MOFs with distinct structures, unique functionalities, and different surface physical and chemical properties into nanofibers by electrospinning. And indeed the compatibility between the MOF nanoparticles and the polymer binders as well as the controllability of the fiber morphology are largely unexplored. All of these are critical for studying the interactions of MOFs with the targeted solid pollutants and the surface chemistry of the MOF filters. Here, we tuned the morphologies (fiber diameter, thickness, and particle dispersion), surface functionalities, and porosity of the filters and investigated the compatibility between MOFs and polymers. Besides, by controlling the particle size and morphology of different MOF crystals, a high loading of 60 wt % can be achieved in the polymer matrix without particle aggregation. The tunable properties of such composite filters (noted as MOFilters) would make them promising candidates for pollutants removal (Figure 1b). As shown in Figure 1c, the pollutants can be captured by MOFilters via three mechanisms: (1) binding to the open metal sites on MOFs; (2) interacting with the functional groups on MOFs and/or polymers; (3) electrostatic interactions with MOF nanocrystals. We used the obtained composite filters as a platform to explore the interactions between MOFs and the pollutants (particulate matter and sulfur dioxide) and try to find the main driving forces that may guide the syntheses of new MOFs and MOFilters with desired filtration capability. Eventually, we hope to propose a general procedure to turn MOF powders into air filters for an all-in-one pollution control strategy.

A series of four MOFs were selected and embedded within three polymers: polyacrylonitrile (PAN), polystyrene (PS), and polyvinylpyrrolidone (PVP), respectively, to give nanofibrous filters. These MOFs were chosen due to their diverse topologies and functionalities: ZIF-8 possesses large cavities with narrow windows and a high ζ potential; UiO-66-NH_2 encompasses polar and base functional groups with a highly stable structure; MOF-199 is comprised of Cu paddle-wheel SBUs linked by a tritopic organic linker with open metal sites; Mg-MOF-74 incorporates both open metal sites and polar functionalities with one-dimensional channels. The MOF/polymer electrospinning solution was prepared by a "priming" technique. Specifically, a small portion of corresponding polymer, PAN, PS, was first added to the MOF dispersion to form a polymer coating on the particles, thus improving the adhesion and preventing aggregation, and then rest of the polymer was added. Besides free-standing filters, the fibrous layers can also be produced onto readily available and cheap substrates such as stainless-steel wire mesh and poly(ethylene terephthalate) nonwoven fabric (Figure S2).

The structures of the polymers and MOFs employed, together with the characteristics of the MOFs are shown in Figure 2a. Besides, the photos and SEM images of the pristine PAN and PS filters along with eight MOFilters supported on flexible nonwoven fabrics are presented. The particle sizes of MOFs were tuned in the nanoscale to ensure their compatibility and dispersion in the polymer fibers (Figure S3). By adjusting the electrospinning parameters such as applied electric voltage and flow rate of the solution, the selected four MOFs can all be spun into fiber mats. As can be seen in Figures 2b, S4, and S5, MOF nanoparticles are well dispersed in the polymers without obvious aggregation even at a high loading of 60 wt %. PAN, PS, and PVP were used as the carrier polymers, and high loadings of MOFs can be achieved in these matrices without reducing the flexibility of thus-obtained filters (Figures S6 and S7). The diameter of the fibers can be tuned in a wide range from 200 nm to 1 μm by adjusting the PAN concentration (6−10 wt %) and MOF loading (20−60 wt %) (Figures 2b, S8, and S9). The PXRD patterns of these MOFilters all, as expected, show that the MOF structures are intact (Figure S10), and N_2 sorption isotherms (Figures S11−S13) demonstrate that the integration of MOF largely improve the porosity and surface area of the original polymer filter. For example, pure PAN filter possesses a BET surface area of 115 m^2/g that is improved to 1024 m^2/g after incorporating ZIF-8 nanoparticles with a mass ratio of 60 wt %.

The nonwoven supported MOFilters (with 20 wt % MOF loading) were employed to remove particulate matter in both simulated and really hazy environments in Beijing. Nanoparticles of aluminum oxide (Al_2O_3), a common inorganic filler, were tested as the benchmark material. As shown in a pioneering study, nanofibrous PAN is believed to be an excellent filter for PM capture.[40] Thus, we chose it as the matrix for MOFilters. Figure 3a demonstrates the removal efficiencies of the filters tested on hazy days in Beijing ($PM_{2.5}$ = 350 μg/m^3, PM_{10} = 720 μg/m^3, RH = 58.6%, and T = 23.5 °C). All the MOFilters show better

DOI: 10.1021/jacs.6b02553
J. Am. Chem. Soc. 2016, 138, 5785−5788

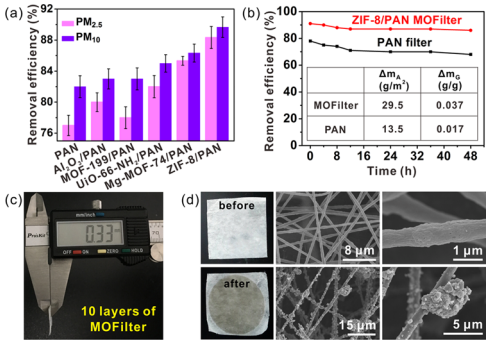

Figure 3. (a) Particulate matter removal efficiencies of PAN filter, Al_2O_3/PAN filter and PAN-MOFilters tested on hazy days in Beijing (T = 23.4 °C, RH = 58.6%, $PM_{2.5}$ = 350 $\mu g/m^3$, PM_{10} = 720 $\mu g/m^3$). Error bar represents the standard deviation of the results from triplicate tests. (b) Long-term $PM_{2.5}$ removal efficiencies of PAN filter and ZIF-8/PAN MOFilter (inset is the gravimetric and areal mass change of the filters before and after PM capture). (c) The thickness of 10 layers of ZIF-8/PAN MOFilter measured by a caliper. (d) Photos and SEM images of the ZIF-8/PAN MOFilter before and after PM capture.

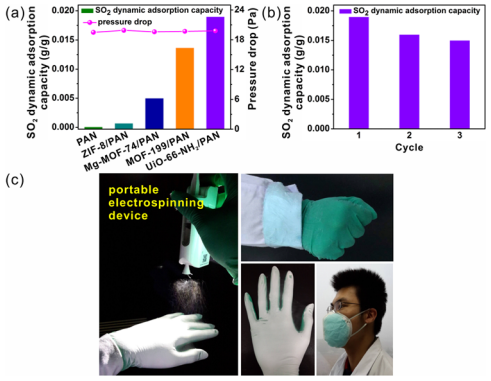

Figure 4. (a) SO_2 dynamic adsorption of PAN filter and PAN-MOFilters at 25 °C with a 100 ppm of SO_2/N_2 flow at the rate of 50 mL/min. (b) Cycle performance of UiO-66-NH_2/PAN MOFilter after regenerating under a N_2 flow rate of 50 mL/min at 25 °C. (c) Photos of MOFilters fabricated on gloves, coats, and masks.

performance than the PAN filter fabricated in the same way, and the higher efficiencies stem from the unique properties endowed by MOFs. Among them, the ZIF-8/PAN MOFilter outperforms others and presents the highest removal efficiency for both $PM_{2.5}$ (88.33 ± 1.52%) and PM_{10} (89.67 ± 1.33%), followed by Mg-MOF-74/PAN, UiO-66-NH_2/PAN, Al_2O_3/PAN, MOF-199/PAN, and PAN.

To elucidate the driving forces of the PM onto filters, we further measured the ζ potential of each sample which was dispersed in ethanol. And the ζ potentials of ZIF-8, Mg-MOF-74, UiO-66-NH_2, MOF-199, and Al_2O_3 are 47.5, 22.9, 39.9, 3.1, and 19.0 mV, respectively. It is clear that the surface charge of MOFs plays a key role in enhancing the adhesion of the PM onto the hybrid fibers. According to a recent research, the main compositions of $PM_{2.5}$ in Beijing are organic matter, nitrate, sulfate, ammonium, chloride, and elemental carbon.[7] Owing to the existence of various ions and water vapor, the particulate matter is highly polar. The unbalanced metal ions on the surface and defects of these MOFs offer the positive charge and thus can polarize the surface of PM improving the electrostatic interactions. However, Mg-MOF-74/PAN MOFilter with a mediocre electrostatic property gives a relative high removal capacity ($PM_{2.5}$ 85.33 ± 0.58%, PM_{10} 86.35 ± 1.16%), which is probably the result of the highly polar hydroxyl groups and the open metal sites. The ζ potentials of the Al_2O_3 and Mg-MOF-74 are on the same level, and the weaker PM capture capability of the former can be attributed to the lack of these additional functional groups and sites. Given the fact that the open metal sites can be easily saturated by water vapor when exposed in humid air (RH = 58.6%), these sites should not be fully accessible. And this can explain the less efficient performance of MOF-199/PAN MOFilter. The high efficiency of ZIF-8/PAN MOFilter can be maintained even after 48 h exposure to polluted air (Figure 3b). A more remarkable mass change occurred in ZIF-8/PAN MOFilter (29.5 g/m^2 or 0.037 g/g, note that the substrate weight is included in the weight of the filter) after PM capture (the inset of Figure 3b), which is due to its better capture ability and stronger binding affinity. The MOFilter was also employed to capture the particles in cigarette smoke (Figures 1b and S14). The thickness of one layer of ZIF-8/PAN MOFilter with nonwoven support is 33 μm (Figure 3c), and the thin layer makes sure the fresh air is easily passed through. The photos and SEM images of the ZIF-8/PAN MOFilter before and after long-term PM capture are exhibited in Figure 3d. Tiny particles are arrested and attached tightly on the surface of the fibers despite the fact that the openings of the filter are much larger than the particles. In general, the integration of MOFs with diverse characteristics into polymer fibers is proved to be an effective way to strengthen the interactions between filters and PM.

MOF powders may clog the pipes and pose a large gas resistance in practical applications, and these MOFilters may offer a better option to adsorb gases in the dynamic processes. Eight layers of MOFilter (with 60 wt % MOF loading and a total thickness of 320 μm) were exposed to a 100 ppm of SO_2/N_2 flow at a rate of 50 mL/min, and the adsorption capability was calculated according to the downstream concentration change that was recorded using a mass spectrometer (Figures S15 and S16). The dynamic SO_2 adsorption capacities of the PAN-MOFilters are shown in Figure 4a. Without MOF immobilization, the pure PAN filter almost shows no capacity for SO_2 adsorption. ZIF-8/PAN MOFilter exhibited better performance because of the high surface area. Remarkable improvements were made by UiO-66-NH_2/PAN (0.019 g/g) and MOF-199/PAN (0.014 g/g) MOFilter, suggesting that the functionalities such as amines and open sites are crucial for kinetic adsorption of acidic polar gas species. Furthermore, these MOFilters show a very low resistance to the gas flow, and the pressure drop at the flow rate of 50 mL/min is as low as 20 Pa. After SO_2 adsorption, the UiO-66-NH_2/PAN MOFilter was regenerated under N_2 flow at 25 °C, and the results shown in Figure 4b indicate that the MOFilter can be reused and the adsorption ability remains largely unchanged. We also further humidified the MOFilters in air at the relative humidity of 60% and tested their dynamic SO_2 adsorption capacities (Figure S17). The structures of the MOF crystals within the filters remained intact after PM capture and SO_2 adsorption (Figure S18). These results indicate that the incorporation of MOFs into nanofibers by electrospinning is a facile way to furnish the polymeric materials with porosity and distinctive properties. The introduction of the portable electrospinning device makes the fabrication process even more convenient. As a proof-of-concept, Figure 4c shows that the MOFilters can be fabricated on various substrates such as lab coats, rubber gloves, and masks, which greatly expands the applications of the filter. For example, before entering some hazardous environment, one can quickly transfer an ordinary coat into a protective suit by depositing certain MOFilters.

DOI: 10.1021/jacs.6b02553
J. Am. Chem. Soc. 2016, 138, 5785−5788

In conclusion, we have designed a series of versatile and cost-effective MOFilters by processing MOFs into nanofibrous filters. Furthermore, these filters with high loadings of MOF particles (up to 60 wt %) can be casted on various substrates. The interactions between MOFs and pollutants including particulate matter and toxic gases are studied. The MOFilters with a thickness of 33 μm can easily capture the PM in a real air-polluted environment with high efficiency ($PM_{2.5}$ 88.33 ± 1.52% and PM_{10} 89.67 ± 1.33%). Also these MOFilters can effectively and selectively adsorb toxic gases such as SO_2 when exposed in a stream of SO_2/N_2 mixture (100 ppm of SO_2), showing a capacity of 0.019g/g with exceptionally low pressure drop of 20 Pa under a flow rate of 50 mL/min. Such hierarchical composite meshes possess large openings allowing the unhindered airflow. The functionalized micropores of MOFs for selective gas capture and controlled surface chemistry of the electrospun MOF nanofibers for efficient PM capture, making MOFilters a promising comprehensive protective material in air pollution control.

■ ASSOCIATED CONTENT

Supporting Information

The Supporting Information is available free of charge on the ACS Publications website at DOI: 10.1021/jacs.6b02553.

Experimental details and data (PDF)

■ AUTHOR INFORMATION

Corresponding Author

*bowang@bit.edu.cn

Notes

The authors declare no competing financial interest.

■ ACKNOWLEDGMENTS

This work was financially supported by the 973 Program 2013CB834704; Provincial Key Project of China (grant no. 7131253); the National Natural Science Foundation of China (grant nos. 21471018, 21404010, 21201018, 21490570); 1000 Plan (Youth).

■ REFERENCES

(1) Lelieveld, J.; Evans, J. S.; Fnais, M.; Giannadaki, D.; Pozzer, A. *Nature* **2015**, *525*, 367.

(2) Fiore, A. M.; Naik, V.; Spracklen, D. V.; Steiner, A.; Unger, N.; Prather, M.; Bergmann, D.; Cameron-Smith, P. J.; Cionni, I.; Collins, W. J.; Dalsoren, S.; Eyring, V.; Folberth, G. A.; Ginoux, P.; Horowitz, L. W.; Josse, B.; Lamarque, J. F.; MacKenzie, I. A.; Nagashima, T.; O'Connor, F. M.; Righi, M.; Rumbold, S. T.; Shindell, D. T.; Skeie, R. B.; Sudo, K.; Szopa, S.; Takemura, T.; Zeng, G. *Chem. Soc. Rev.* **2012**, *41*, 6663.

(3) Brunekreef, B.; Holgate, S. T. *Lancet* **2002**, *360*, 1233.

(4) Kampa, M.; Castanas, E. *Environ. Pollut.* **2008**, *151*, 362.

(5) Hoek, G.; Krishnan, R. M.; Beelen, R.; Peters, A.; Ostro, B.; Brunekreef, B.; Kaufman, J. D. *Environ. Health* **2013**, *12*, 43.

(6) Seaton, A.; Macnee, W.; Donaldson, K.; Godden, D. *Lancet* **1995**, *345*, 176.

(7) Huang, R.-J.; Zhang, Y.; Bozzetti, C.; Ho, K.-F.; Cao, J.-J.; Han, Y.; Daellenbach, K. R.; Slowik, J. G.; Platt, S. M.; Canonaco, F.; Zotter, P.; Wolf, R.; Pieber, S. M.; Bruns, E. A.; Crippa, M.; Ciarelli, G.; Piazzalunga, A.; Schwikowski, M.; Abbaszade, G.; Schnelle-Kreis, J.; Zimmermann, R.; An, Z.; Szidat, S.; Baltensperger, U.; Haddad, I. E.; Prévôt, A. S. H. *Nature* **2014**, *514*, 218.

(8) Rohrer, F.; Lu, K.; Hofzumahaus, A.; Bohn, B.; Brauers, T.; Chang, C.-C.; Fuchs, H.; Haeseler, R.; Holland, F.; Hu, M.; Kita, K.; Kondo, Y.; Li, X.; Lou, S.; Oebel, A.; Shao, M.; Zeng, L.; Zhu, T.; Zhang, Y.; Wahner, A. *Nat. Geosci.* **2014**, *7*, 559.

(9) Lu, Z.; Streets, D. G.; Zhang, Q.; Wang, S.; Carmichael, G. R.; Cheng, Y. F.; Wei, C.; Chin, M.; Diehl, T.; Tan, Q. *Atmos. Chem. Phys.* **2010**, *10*, 6311.

(10) Furukawa, H.; Cordova, K. E.; O'Keeffe, M.; Yaghi, O. M. *Science* **2013**, *341*, 1230444.

(11) Férey, G.; Millange, F.; Morcrette, M.; Serre, C.; Doublet, M. L.; Greneche, J. M.; Tarascon, J. M. *Angew. Chem., Int. Ed.* **2007**, *46*, 3259.

(12) Zhou, H. C.; Kitagawa, S. *Chem. Soc. Rev.* **2014**, *43*, 5415.

(13) Murray, L. J.; Dincă, M.; Long, J. R. *Chem. Soc. Rev.* **2009**, *38*, 1294.

(14) Li, J. R.; Sculley, J.; Zhou, H. C. *Chem. Rev.* **2012**, *112*, 869.

(15) Banerjee, R.; Phan, A.; Wang, B.; Knobler, C.; Furukawa, H.; O'Keeffe, M.; Yaghi, O. M. *Science* **2008**, *319*, 939.

(16) Barea, E.; Montoro, C.; Navarro, J. A. *Chem. Soc. Rev.* **2014**, *43*, 5419.

(17) Zhao, J.; Nunn, W. T.; Lemaire, P. C.; Lin, Y.; Dickey, M. D.; Oldham, C. J.; Walls, H. J.; Peterson, G. W.; Losego, M. D.; Parsons, G. N. *J. Am. Chem. Soc.* **2015**, *137*, 13756.

(18) Britt, D.; Tranchemontagne, D.; Yaghi, O. M. *Proc. Natl. Acad. Sci. U. S. A.* **2008**, *105*, 11623.

(19) DeCoste, J. B.; Peterson, G. W. *Chem. Rev.* **2014**, *114*, 5695.

(20) Wisser, D.; Wisser, F. M.; Raschke, S.; Klein, N.; Leistner, M.; Grothe, J.; Brunner, E.; Kaskel, S. *Angew. Chem., Int. Ed.* **2015**, *54*, 12588.

(21) Kumar, P.; Kim, K.-H.; Kwon, E. E.; Szulejko, J. E. *J. Mater. Chem. A* **2016**, *4*, 345.

(22) Khan, N. A.; Jhung, S. H. *Angew. Chem., Int. Ed.* **2012**, *51*, 1198.

(23) Peterson, G. W.; Rossin, J. A.; DeCoste, J. B.; Killops, K. L.; Browe, M.; Valdes, E.; Jones, P. *Ind. Eng. Chem. Res.* **2013**, *52*, 5462.

(24) Hamon, L.; Serre, C.; Devic, T.; Loiseau, T.; Millange, F.; Férey, G.; De Weireld, G. *J. Am. Chem. Soc.* **2009**, *131*, 8775.

(25) McKinlay, A. C.; Xiao, B.; Wragg, D. S.; Wheatley, P. S.; Megson, I. L.; Morris, R. E. *J. Am. Chem. Soc.* **2008**, *130*, 10440.

(26) Shimomura, S.; Higuchi, M.; Matsuda, R.; Yoneda, K.; Hijikata, Y.; Kubota, Y.; Mita, Y.; Kim, J.; Takata, M.; Kitagawa, S. *Nat. Chem.* **2010**, *2*, 633.

(27) López-Maya, E.; Montoro, C.; Rodriguez-Albelo, L. M.; Aznar Cervantes, S. D.; Lozano-Perez, A. A.; Cenis, J. L.; Barea, E.; Navarro, J. A. *Angew. Chem., Int. Ed.* **2015**, *54*, 6790.

(28) Peterson, G. W.; Wagner, G. W. *J. Porous Mater.* **2014**, *21*, 121.

(29) Mondloch, J. E.; Katz, M. J.; Isley, W. C., III; Ghosh, P.; Liao, P.; Bury, W.; Wagner, G. W.; Hall, M. G.; DeCoste, J. B.; Peterson, G. W.; Snurr, R. Q.; Cramer, C. J.; Hupp, J. T.; Farha, O. K. *Nat. Mater.* **2015**, *14*, 512.

(30) Bétard, A.; Fischer, R. A. *Chem. Rev.* **2012**, *112*, 1055.

(31) Qiu, S.; Xue, M.; Zhu, G. *Chem. Soc. Rev.* **2014**, *43*, 6116.

(32) Bradshaw, D.; Garai, A.; Huo, J. *Chem. Soc. Rev.* **2012**, *41*, 2344.

(33) Yao, J.; Wang, H. *Chem. Soc. Rev.* **2014**, *43*, 4470.

(34) Erucar, I.; Yilmaz, G.; Keskin, S. *Chem. - Asian J.* **2013**, *8*, 1692.

(35) Li, W.; Zhang, Y.; Li, Q.; Zhang, G. *Chem. Eng. Sci.* **2015**, *135*, 232.

(36) Tanh Jeazet, H. B.; Staudt, C.; Janiak, C. *Dalton Trans.* **2012**, *41*, 14003.

(37) Zornoza, B.; Tellez, C.; Coronas, J.; Gascon, J.; Kapteijn, F. *Microporous Mesoporous Mater.* **2013**, *166*, 67.

(38) Greiner, A.; Wendorff, J. H. *Angew. Chem., Int. Ed.* **2007**, *46*, 5670.

(39) Li, D.; Xia, Y. N. *Adv. Mater.* **2004**, *16*, 1151.

(40) Liu, C.; Hsu, P. C.; Lee, H. W.; Ye, M.; Zheng, G.; Liu, N.; Li, W.; Cui, Y. *Nat. Commun.* **2015**, *6*, 6205.

(41) Gong, G.; Zhou, C.; Wu, J.; Jin, X.; Jiang, L. *ACS Nano* **2015**, *9*, 3721.

(42) Rose, M.; Böhringer, B.; Jolly, M.; Fischer, R.; Kaskel, S. *Adv. Eng. Mater.* **2011**, *13*, 356.

(43) Ostermann, R.; Cravillon, J.; Weidmann, C.; Wiebcke, M.; Smarsly, B. M. *Chem. Commun.* **2011**, *47*, 442.

(44) Wu, Y.-n.; Li, F.; Liu, H.; Zhu, W.; Teng, M.; Jiang, Y.; Li, W.; Xu, D.; He, D.; Hannam, P.; Li, G. *J. Mater. Chem.* **2012**, *22*, 16971.

(45) Ren, J.; Musyoka, N. M.; Annamalai, P.; Langmi, H. W.; North, B. C.; Mathe, M. *Int. J. Hydrogen Energy* **2015**, *40*, 9382.

(46) Liu, C.; Wu, Y. N.; Morlay, C.; Gu, Y.; Gebremariam, B.; Yuan, X.; Li, F. *ACS Appl. Mater. Interfaces* **2016**, *8*, 2552.

DOI: 10.1021/jacs.6b02553
J. Am. Chem. Soc. 2016, 138, 5785−5788